

# **TITLE**

by Natasha Louise Hopkins

**Master of Biology (Honours), Molecular Cell Biology**  
University of York, UK

**Project Director**  
Prof. Robert J White

**Examination Date**  
17 April, 2023

**Word Count**

Abstract:

Main:



# Contents

<b>Introduction</b>	<b>1</b>
tRNAs and Carcinogenesis . . . . .	1
ER+ Breast Cancer and FOXA1 . . . . .	2
<b>Materials &amp; Methods</b>	<b>3</b>
ChIP-seq Data from NCBI . . . . .	3
EaSeq for the Quantification of Signals at tDNAs . . . . .	3
Motif Analysis . . . . .	4
Statistics . . . . .	4
ChIP-Seq and ChIP-qPCR . . . . .	4
<b>Results</b>	<b>6</b>
Localisation of FOXA1 and H3k27ac at tRNA genes in MCF-7 cells . . . . .	6
FOXA1 alters H3K27ac binding levels . . . . .	8
tDNAs are activated by FOXA1 OE . . . . .	8
FOXA1 OE influences the binding location of FOXA1 and H3K27ac . . . . .	11
Motif Analysis . . . . .	11
What? . . . . .	11
Figure 5 . . . . .	11
<b>Discussion</b>	<b>16</b>
<b>Conclusion</b>	<b>17</b>
<b>References</b>	<b>17</b>

# TITLE

Natasha L. Hopkins

Abstract

1 Words

---

## Introduction

### tRNAs and Carcinogenesis

In Eukaryotes, transcription of DNA is tightly-regulated by three RNA polymerase enzymes. RNA Polymerase III (Pol III), the largest of the three at 17-subunits<sup>1</sup>, produces a series of short non-coding RNAs, including U6 snRNA, 5S rRNA and transfer RNA (tRNA)<sup>2</sup>. Approximately 80% of Pol III binding resides at tRNAs<sup>3</sup> – adapters required to translate mRNAs into the amino acid protein sequence. Initiation of tRNA transcription requires the binding of TFIIIC, a multi-subunit complex, to internal tRNA promoters, the A and B boxes, which are located downstream of the transcription start site<sup>4-6</sup>. This protein-protein interaction enables the recruitment of the TFIIIB promoter, composed of the TATA-box-binding protein (TBP), BDP1, and BRF1 polypeptides<sup>7</sup>. TFIIIB occupies the region upstream of the transcription start site and binds to Pol III directly through BRF<sup>8</sup>, positioning it at the initiation region<sup>9</sup>.

Protein synthesis by Pol III dictates cell growth and proliferation<sup>10-12</sup>. Deregulation of Pol II is associated with a range of cancers<sup>13,14</sup>, including ovarian and breast<sup>15,16</sup>. In healthy cells, tumour suppressors such as RB and p52 regulate Pol III transcription. This is achieved through binding to TFIIIB, blocking interactions to both TFIIIC and Pol III<sup>17-20</sup>. Loss of RB and p53 in transformed cells consequently enhances Pol III transcription. Contrarily, induction of onco-proteins MAP kinase Erk or c-Myc may stimulate Pol II expression through interactions with TFIIIB<sup>21,22</sup>. The relationship between Pol III and cell transformation directly implicates tRNAs in carcinogenesis. ~~Tumour cells contain tRNAs that are absent from the normal tissue of origin<sup>23</sup>.~~

Specific tRNAs have also been shown to drive cancer progression<sup>24</sup>. For instance, overexpression of the transcription initiator tRNA<sub>i</sub><sup>Met</sup> alters global tRNA expression, increasing cell activity and proliferation<sup>25</sup>, as demonstrated in melanoma cells<sup>26</sup>. Reporter assays revealed that some tRNA genes (tDNAs) act as insulators by restricting spread of heterochromatin<sup>27-29</sup>.

## ER+ Breast Cancer and FOXA1

In 2020, female breast was the most commonly diagnosed cancer worldwide with over 2.2 million cases<sup>30</sup>. Estrogen Receptor (ER) drives 75% of breast cancers cancers<sup>31</sup>. Presence of ER is generally prognostic of positive outcomes, due to it's use as a therapeutic target. Estrogen levels are lowered using endocrine therapies with aromatase inhibitors; fulvestrant, a selective estrogen receptor down regulator (SERD) which binds and degrades the ER, and tamoxifen, a selective estrogen receptor modulator (SERM) which competes with estrogen for binding to ER<sup>32</sup>. However, resistance to endocrine therapy occurs in 40-50% of tumours from 5 years of diagnosis<sup>33</sup>.

Forkhead box A1 (FOXA1) is a pioneer factor capable of directly initiating chromatin opening, facilitating binding of ER and other transcription factors<sup>34-37</sup>. Early studies demonstrated that FOXA1 maps to ~50% of ER-chromatin binding sites. Furthermore, silencing of FOXA1 reduces ~95% ER binding events<sup>36,38</sup>.

~~FOXA1 is an established growth inhibitor in both ER+ breast cancer cells and ER- cells with forced ER expression<sup>39</sup>. Though binding to p27<sup>kip1</sup>, FOXA1 is also involved in recruiting tumour suppressor BRCA1<sup>40-42</sup>.~~

The presence of FOXA1 determines treatment response in ER+ breast cancer; FOXA1 is associated with positive prognoses following treatment with tamoxifen<sup>38,43</sup>. However, FOXA1 and ER has also been found to be overexpressed in some ER+ endocrine resistant breast cancer lines<sup>44</sup>. Studies have shown that amplification of FOXA1 promotes endocrine-resistant growth and invasiveness by reprogramming the ER-transcriptome<sup>45</sup>.

Aberrant expression of tRNAs in breast cancers has been observed in several studies<sup>13,14,16,46</sup>. Upon stimulation by estrogen, ER+ breast cancer cells undergo extensive transcriptional changes, upregulating 90% of tRNA genes<sup>46</sup>. Additionally, ER amplifies alcohol-induced deregulation of tRNA<sup>Leu</sup> by in MCF-7 cells<sup>47</sup>.

As ER+ BC is reliant on FOXA1, the aim of this study was to determine whether FOXA1 elevates tDNA expression. To achieve this, a bioinformatics approach was taken to analyse publicly available FOXA1 and H3K27ac ChIP-seq datasets from Fu et al. (2019)<sup>48</sup> in the context of the MCF-7 cell line. Here, identification of FOXA1 and H3K27ac co-localisation at tDNAs may provide insight into FOXA1's relevance in the altered tRNA expression associated with poor prognosis in ER+ breast cancer.

---

# Materials & Methods

## ChIP-seq Data from NCBI

FOXA1 and H3K27ac ChIP-seq was performed on genetically modified MCF7L cells (*insertion, using a lentiviral cDNA delivery system to express Dox-inducible FOXA1*) by the lab of Xiaoyong Fu, Baylor College of Medicine, and made publicly available on Dec 18 2019<sup>48</sup>. Datasets were deposited into the National Centre for Biotechnology Information (NCBI) Sequence Read Archive (SRA) Run Selector<sup>49</sup> under the accession number PRJNA513000 (Available at <https://www.ncbi.nlm.nih.gov/sra> ; Table 1). Using “Genetic Manipulation Tools” within the Galaxy<sup>50</sup> environment (v 23.0.rc1), SRAs were converted to FastQ files. FastQ files were then aligned to the human genome assembly GRCh37 (hg19) by Bowtie2 (v 2.5.0)<sup>51</sup> to output BAM files.

**Table 1.** Publicly available ChIP-seq SRA files aquired from the NCBI SRA database (accession no. PRJNA512997).

Experiment	SRA	Factor	Tissue	Assembly
PRJNA513000	SRR8393424	FOXA1	MCF-7LP	GRCh37 (Hg19)
	SRR8393425			
	SRR8393426			
	SRR8393427	H3K27ac		
	SRR8393428			
	SRR8393431	None (input)		
	SRR8393432			

## EaSeq for the Quantification of Signals at tDNAs

BAM files were uploaded into EaSeq (v1.111) as “Datasets” using the standard settings for Chip-seq data. GRCh37 (hg19) tRNA sequences (n = 606) were downloaded as a “Geneset” from the UCSC Table Browser<sup>52</sup>, (available at <https://genome.ucsc.edu>). High-confidence tRNAs (n = 416) identified by the GtRNAdb<sup>53</sup> were extracted as a “Regionset”.

Signal peak intensities surrounding tRNAs were quantified using the EaSeq “quantify” tool. Here the default settings “Normalize to reads per million” and “Normalize counts to DNA-fragments” were left checked. The default setting “Normalise to a signal of 1000 bp” was unchecked. The window size was offset ±500bp from the start of each tRNA gene. Generated values are referred to as “Q-values”.

To quantify upstream and downstream signals, the “quantify” tool was used with adjusted window sizes. The upstream region was defined as 500 bp preceding and the first nucleotide of tRNA loci. Thus, the start position was offset to 0 bp, and the end position was offset to -500

bp. The downstream region constitutes the 500 bp region beginning with the first nucleotide of tRNA gene body. The start position was offset to 1 bp, and the end position was offset to 500 bp. Following quantification, tRNA binding events were arranged in ascending order of -Dox Q-value and visualised as heatmaps. Data was also visualised with the “heatmap”, “average”, “overlay”, and “fill-track” tools (Figure 1). EaSeq<sup>54</sup> is available at <http://easeq.net>.

## Motif Analysis

Motif analysis was carried out in active +Dox tDNA genes which had the largest significant increase in FOXA1 or H3K27ac Q-values following ChIP-seq.

!!1!!!!1 !!!!!!1

Multiple EM for Motif Elicitation ChIP (MEME) Suite

## Statistics

Statistical analysis and visualisation was generated with R<sup>55</sup> (v 4.2.3) with the tidyverse<sup>56</sup> and ggpubr<sup>57</sup> packages.

Group differences were determined by Mann-Whitney U, Wilcoxon signed-rank test, and the Chi-squared test.

## ChIP-Seq and ChIP-qPCR

MCF-7L cells were grown in PRF medium with 5% CS-FBS and /+ Dox. Cells were cross-linked with 1% formaldehyde for 10 mins. Cross-linking was inhibited by quenching (1/20V, 125 mM glycine). Cells were washed in cold PBS and harvested in cold PBS with protease inhibitors (Roche). Pelleted cells were re-suspended in cytosolic and then lysed in nuclear lysis buffer (10-20 min), and sheared at high output (Bioruptor, Diagenode; 4 °C, 30s per sonication cycle for 20 min). Sonicated lysates were cleared by centrifugation (20,000 × g, 10 min) and diluted (4 times) before pre-incubation with protein-A/G beads (Santa Cruz; 4 °C, 30 min).

ChIP was performed by overnight incubation (4 °C) with antibody against human FOXA1 (Abcam, ab23738) or H3K27ac (Active Motif, #39134), followed by an additional incubation with protein-A/G beads (1h). For FOXA1 ChIP-seq, spike-in *Drosophila melanogaster* chromatin was added with the antibody against histone variant H2Av (Active Motif, # 61752). The beads were washed with low and high salt wash buffer, once with LiCl wash buffer (20 mM Tris pH 8.0, 1 mM EDTA, 250 mM LiCl, 1% Nonidet P-40, 1% sodium deoxycholate), and once with TE buffer. DNA was eluted (50 mM NaHCO3 and 1% SDS) and then supplemented with NaCl (300 mM). Cross-links were reversed by incubating overnight (67 °C). RNA was digested at 37 °C with RNase A (0.1 mg/mL, 30 min). DNA was purified with a PCR purification kit (Qiagen).

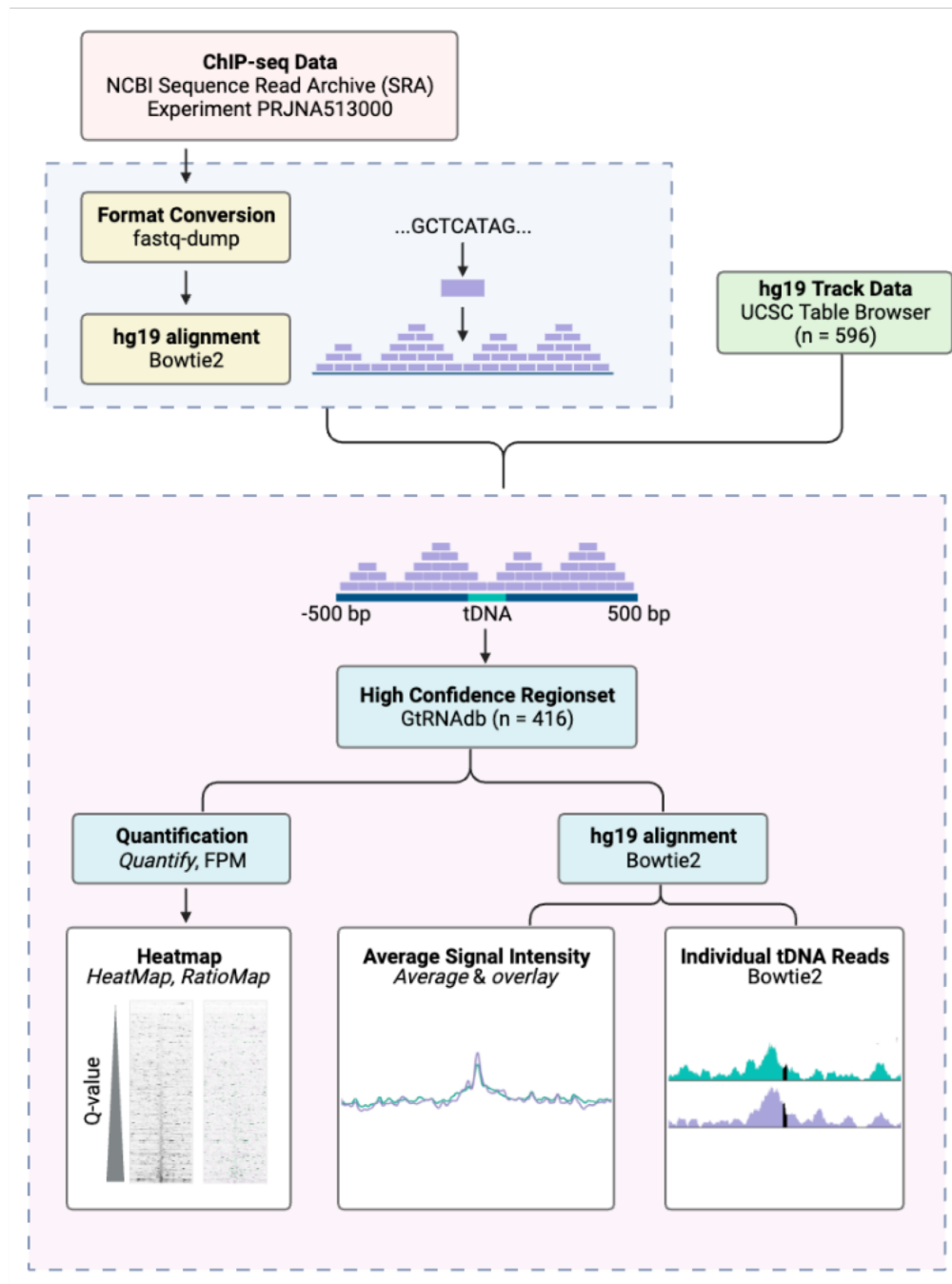


**Figure 1.** Overview of bioinformatic pipeline.

Indexed libraries were prepared from ChIP DNA using the KAPA Hyper Library Preparation Kit (Kapa Biosystems). Libraries were amplified by PCR (12 cycles), and then assessed for size distribution using the 4200 TapeStation High Sensitivity D1000 ScreenTape (Agilent Technologies) and quantified using the Qubit dsDNA HS Assay Kit (ThermoFisher). The indexed libraries were multiplexed, 10 libraries per pool. Real time quantitative PCR (qPCR) was performed using the KAPA Library Quantification Kit (KAPA Biosystems) and then sequenced on the Illumina NextSeq500 using the high-output 75 bp single-read configuration.

---

## Results

### Localisation of FOXA1 and H3k27ac at tRNA genes in MCF-7 cells

Estrogen stimulates the production of tRNAs<sup>46</sup>. The estrogen receptor is dependent on FOXA1; ChIP-seq analysis has shown that FOXA1 reprograms chromatin in MCF-7 cells<sup>58</sup>. To investigate whether FOXA1 enhances tDNA expression, a doxycycline (Dox) inducible OE system in MCF-7 cells was used to achieve FOXA1 OE comparable to endogenous MCF7 tamoxifen-resistant cells (TamR). ChIP-seq analysis was carried out for FOXA1 and H3K27ac; open, H3K27ac denotes accessible chromatin and is used to identify active promoters.

It was expected that FOXA1 would alter tDNA activity. Mapped reads of FOXA1 and H3K27ac binding was quantified (Q-values) relative to  $\pm 500$  bp flanking regions. Binding events were visualised as heatmaps and ordered by increasing -DOX Q-value. This revealed a concentration of FOXA1 and H3k27ac at approximately half of tDNAs, relative to  $\pm 10$  kb flanking regions.

Upon FOXA1 induction, FOXA1 binding increases at a small proportion of tRNAs genes. H3K27ac binding decreases at approximately half of tRNA genes (Figure 2A). This was confirmed by average signal intensity plots of FOXA1 and H3K27ac binding (Figure 2B). Input reads generated minimal peak enrichment (Supplementary Figure X).

FOXA1 density statistically increased in response to FOXA1 induction. Median FOXA1 Q-values were (Figure 2D) increased 10.9% ( $p = 0.021$ ). For H3K27ac, median Q-values decreased by 1.1%, however this change was not statistically significant (Figure 2D).

Peaks were classified as binding events if Q-values exceeded input values ( $\log_2(Q\text{-value fold-change}) > 0$ ) (Figure 2C). Before FOXA1 OE, FOXA1 interacts with 329 tRNA genes and H3K27ac with 293 tRNA genes. The majority of these events are co-binding, with both FOXA1 and H3K27ac binding to 262 tDNAs. Upon FOXA1 OE, the number of FOXA1 binding sites decrease to 319; 40 are lost and 30 are gained, whilst 309 pre-existing sites remained. H3K27ac sites also decrease to 266 tDNAs; 50 are lost and 23 are gained, whilst 239 pre-existing sites remained. Correspondingly, co-binding events lower to 246; 44 are lost and 28 are gained, whilst 230 pre-existing sites remained. Together, these results support the notion that FOXA1 and H3K27ac bind to tDNAs.

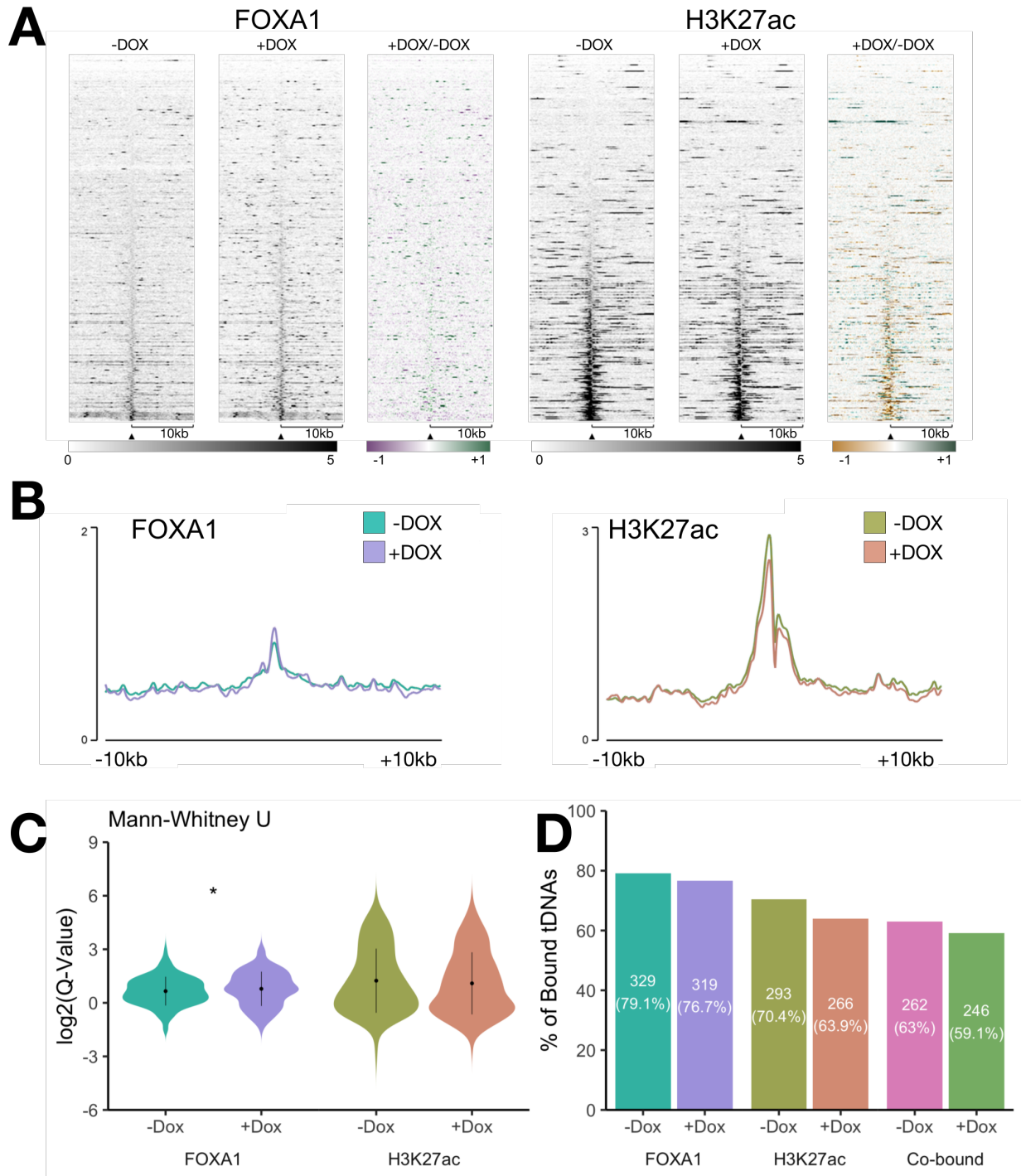


**Figure 2.** Comparisons of FOXA1 and H3K27ac binding at tDNAs, with and without Dox. (A) Heatmaps of FOXA1 and H3K27ac across hg19 tRNA genes in MCF-7 cells. Genes arranged in order of increasing -Dox Q-value. Ratiometric heatmaps represent the log<sub>2</sub> ratio between -Dox and +Dox peaks. Windows represent  $\pm 10\text{kb}$  from the centre of the gene. N = 416. (B) Average signal intensity overlay of FOXA1 and H3K27ac. Windows represent  $\pm 10\text{kb}$  from the centre of the gene. (C) Violin plots of FOXA1 and H3K27ac Q-values within  $\pm 500\text{bp}$  of the gene body. \* $p < 0.05$ . (D) Bar plots of the percentage of cells bound by FOXA1 and H3K27ac.

## **FOXA1 alters H3K27ac binding levels**

To elucidate how FOXA1 impacts tDNA levels, tDNAs that were differently enriched upon FOXA1 OE were categorised as gained (UP) and lost (DN) (fold-change > 1.5,  $P$ -value > 1e-3). This discovered that substantially more tDNAs gained (UP) FOXA1 binding than lost (DN) (96 vs. 62), whilst 258 tDNAs remained relatively unchanged (Figure 3A, left). For H3K27ac, 54 tDNAs gained (UP) and 124 lost (DN) H3K27ac (Figure 3A, right), whereas 236 tDNAs remained relatively unchanged. As expected, Q-values density was significantly increased or decreased at UP and DN tDNAs, respectively (Figure 3B). For FOXA1, median Q-values decreased 42.7% at DN tDNAs, and increased 90% at UP tDNAs. For H3K27ac, median Q-values decreased 26.4% at DN tDNAs, and increased 81.5% at UP tDNAs.

Focusing on UP tDNAs, 95 gain (UP) FOXA1 and 54 gain (UP) H3K27ac (Figure 3C). Of this subset ( $n = 150$ ), 14% gain both FOXA1 and H3K27ac. Examples of exclusive and co-bound tDNAs are shown in Figure 3D.

### SUMMARY

## **tDNAs are activated by FOXA1 OE**

The next step was to investigate the impact of FOXA1 on tDNA activity. Almost half of human tDNAs are silent or poorly expressed<sup>59</sup>. Thus, tDNAs were classified as ‘active’ if H3K27ac Q-values exceeded the median -DOX value ( $Q > 1.808$ ). The Q-value density of inactive tDNAs was somewhat altered ( $p = 0.043$ ), with median FOXA1 Q-values decreasing 4.9% (Figure 4A). The density of active tDNAs did not significantly change, though the median Q-value did decrease 18.9%.

Overexpression of FOXA1 altered the number of active and inactive tDNAs by just 1 (Supplementary Figures X). However, 27 tDNAs became inactive (LOSS) and 26 became activate (GAIN), whilst the activity status of 363 (87.3%) tDNAs remained not changed (NC) (Figure 4B). As expected, the Q-value density of activated (GAIN) tDNAs was changed upon FOXA1 OE (Figure 4C). Q-values increased 65.4% for GAIN tDNAs, decreased 14.2% for LOSS, decreased 8.3% for NC tDNAs. However, these changes were not significant for the last two catagories.

Superimposing GAIN and LOSS tDNAs with UP and DOWN tDNAs (Figure 3C) revealed that, of the 26 tDNAs that become active upon FOXA1 OE, 19 also reasonably gained H3K27ac (H3K27ac UP), and 13 reasonably gain FOXA1 (FOXA1 UP) (Figure 4D). Whereas 16 tDNAs gained both H3K27ac and FOXA1. 9 activated tDNAs gain (UP) both H3K27ac and FOXA1 binding. Examples of activated tDNAs with increased H3K27ac, FOXA1, or both, are shown in Figure 4E.

### SUMMARY

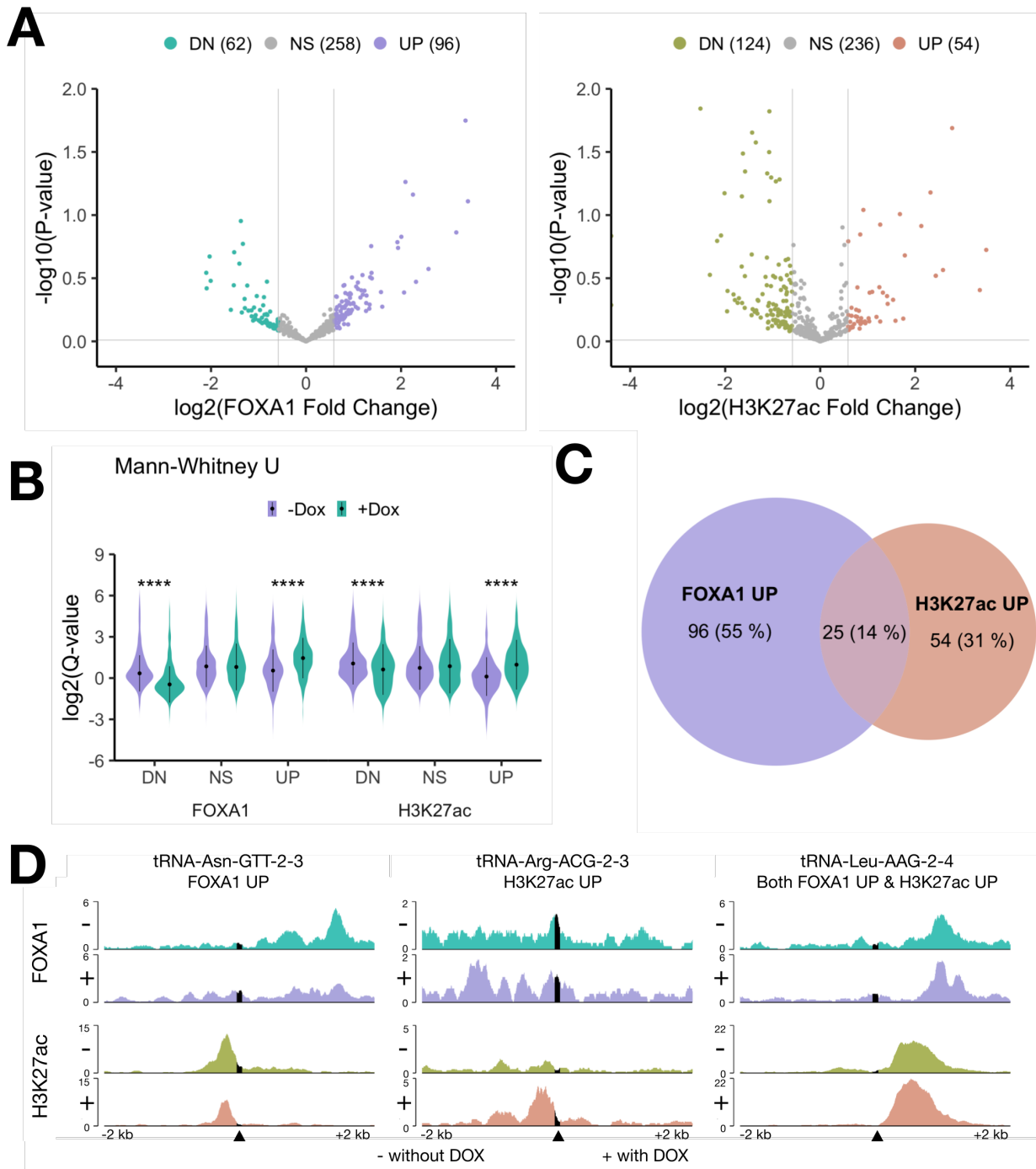


**Figure 3.** FOXA1 OE impacts binding of FOXA1 and H3K27ac at tRNA genes. (A) Volcano plots of FOXA1 ( $n = 416$ ) and H3K27ac ( $n = 414$ ) Q-values in +Dox vs. Dox cells. (Left) The purple and green dots correspond to the regions with UP and DN FOXA1, respectively. (Right) The orange and green dots correspond to the regions with UP and DN H3K27ac, respectively. The threshold for calling was set fold-change  $> 1.5$  and  $P < 1e-3$ . (B) Violin plots of the Q-values of GAIN or LOSS tRNA genes. \*\*\*\* $p < 0.0001$ . (C) Venn diagram representing the overlap between FOXA1 and H3K27ac GAIN regions. (D) Filltrack examples of separate and co-occurring FOXA1 and H3K27ac GAIN events within  $\pm 2$  kb of tDNAs. The black line represents the gene body.

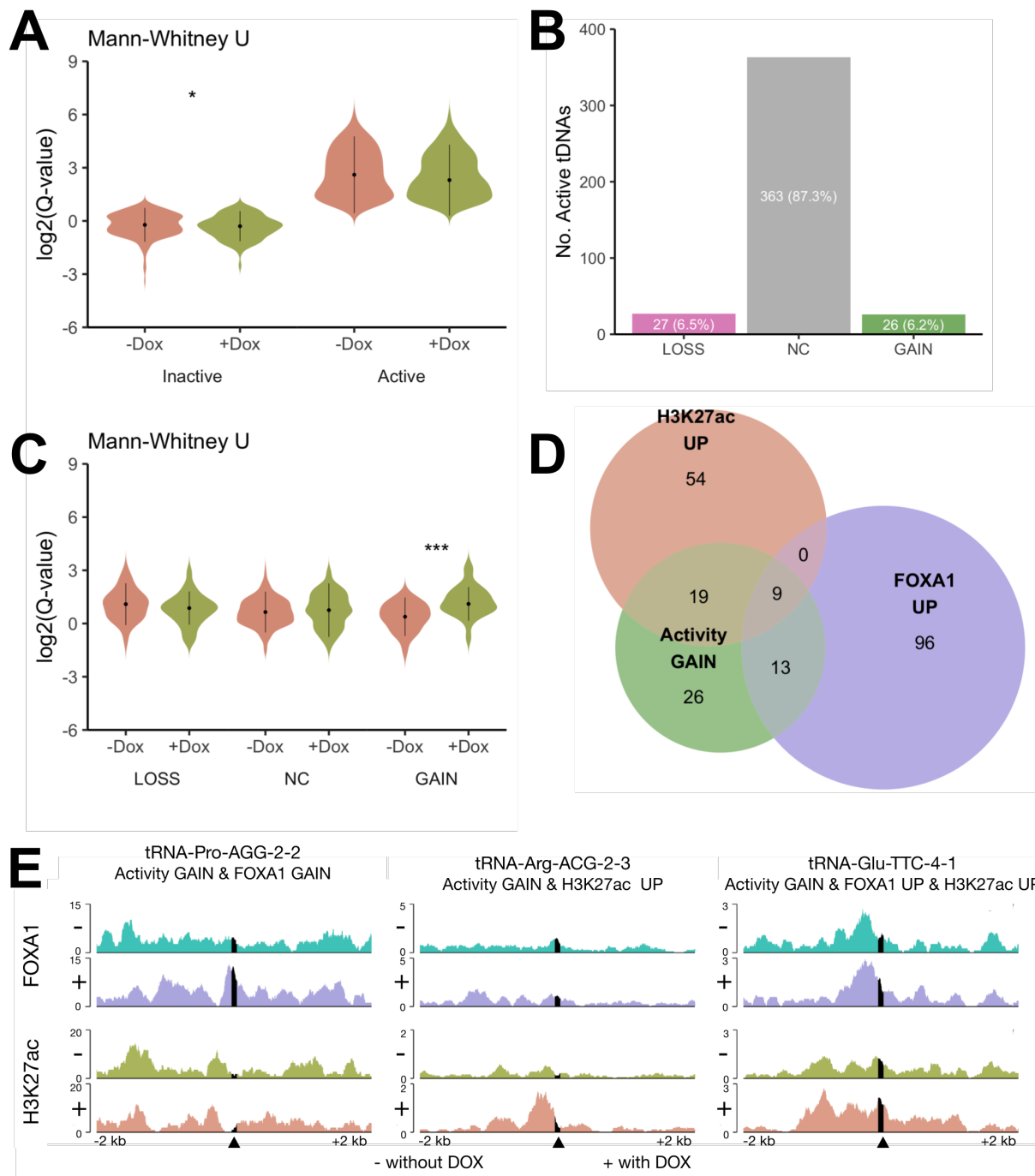


**Figure 4.** (A) Violin plot of H3K27ac Q-values within  $\pm 500$ bp of the gene body of inactive and active tDNAs. \* $p < 0.05$ . (B) Barplot of tDNAs categorised by activity change upon FOXA1 OE. tDNAs are classed as inactivated (LOSS), no-change (NC), and activated(GAIN). (C) Violin plot of tDNA Q-values, categorised as they are in B. \* $p < 0.05$ , \*\* $p < 0.01$ . (D) Venn diagram representing the overlap between tDNAs classed as GAIN and UP. (E) Filltrack examples of co-occurring FOXA1 UP and H3K27ac GAIN events within  $\pm 2$  kb of tDNAs. The black line represents the gene body.

## **FOXA1 OE influences the binding location of FOXA1 and H3K27ac**

To assess FOXA1 and H3K27ac binding preference, the levels of FOXA1 and H3K27ac at upstream and downstream regions was quantified within a  $\pm$  500 bp (Figure 5A). The upstream window was classified as the 500 bp region preceding the tDNA loci, including the the TSS. In contrast, the 500 bp region preceding the TSS defined the downstream region.

FOXA1 was found to be bound at more downstream sites than upstream sites, both with FOXA1 OE and without (-DOX 307 vs 319; +Dox 297 vs 331) (Figure 5B) . However, FOXA1 did not significantly change the number of FOXA1 bound DNAs upstream or downstream (Figure 5C). On the other hand, significantly more H3K27ac binding events occurred downstream (-DOX 284 vs 280; +Dox 276 vs 240) (Figure 5B). This pattern of H3K27ac binding was further perpetuated by FOXA1 OE; Q-values significantly decreased 3.8% upstream and 14.3% downstream (Figure 5C).

## **Motif Analysis**

### **Why?**

### **What?**

- MEME SEA of GAIN UP UP tDNAs (n = 9)
- 27 de novo identified
- A and B box motifs as a control
- p-values
- mention AR motif also enriches/ any other established fox interactions

### **Suggests?**

## **Figure 5**

- Localisation of FOXA1 at individual tDNA genes in MCF-7 cells
- why - tRNAs implicated in cancer
- Largely unchanged
- mention exceptions
- examples of NC, UP, DOWN or 1 example from each family/cluster?

### **Suggests?**

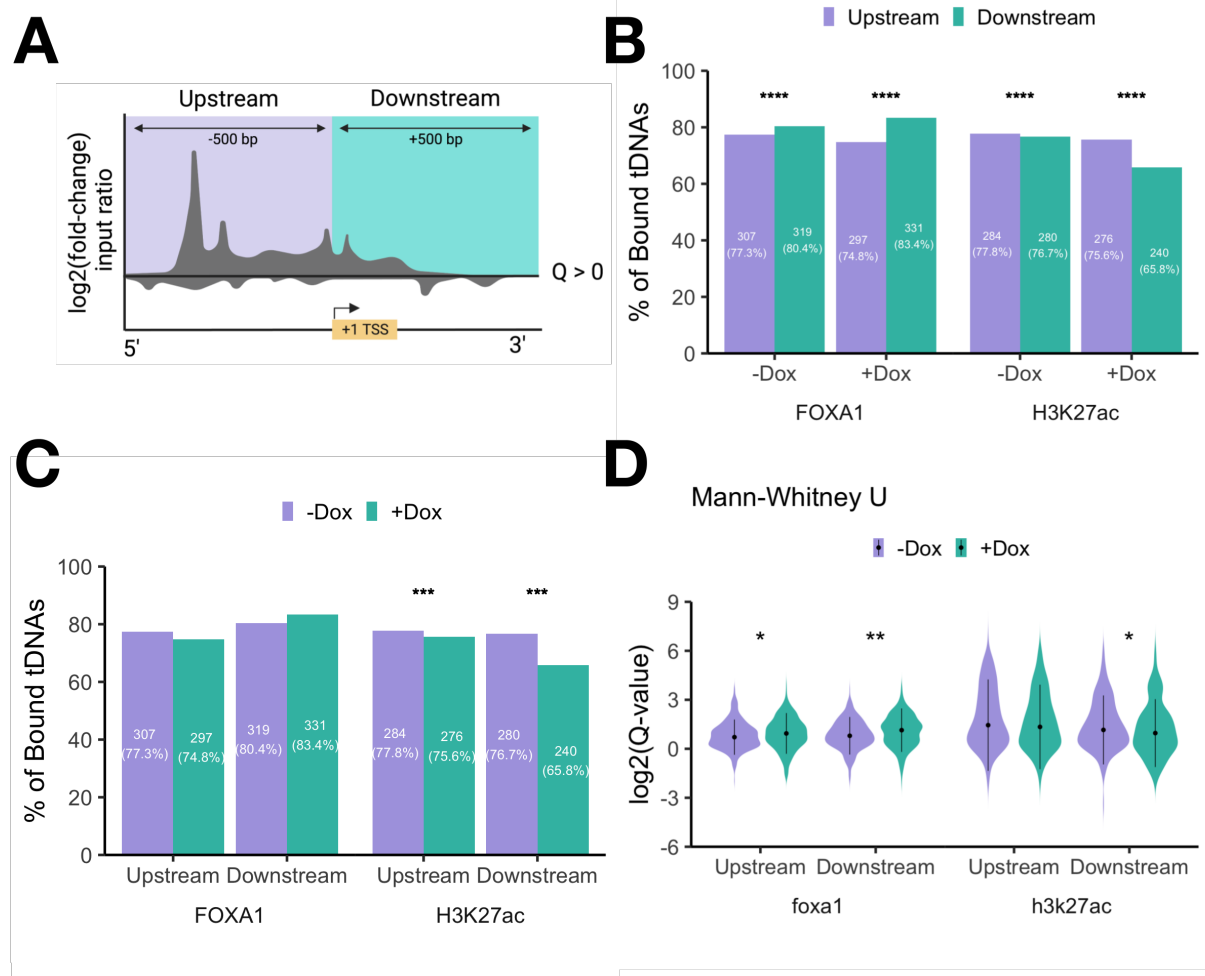
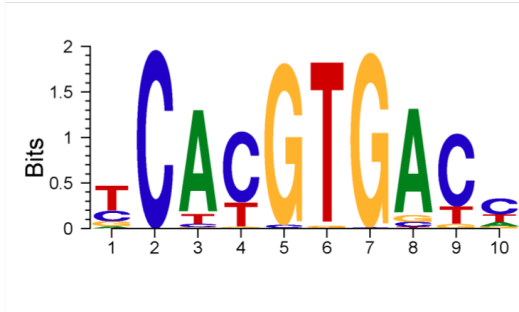
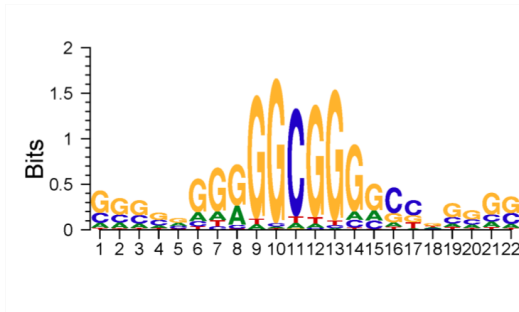


**Figure 5.** (A) Schematic of the independent quantification of the upstream and downstream regions of tDNAs. Windows were confined to the  $\pm 500$  bp, including the gene body. Binding events were counted if Q-values exceeded the input values. (B) Violin plot of the upstream and downstream Q-values for FOXA1 and H3K27ac, with or without Dox. (C)

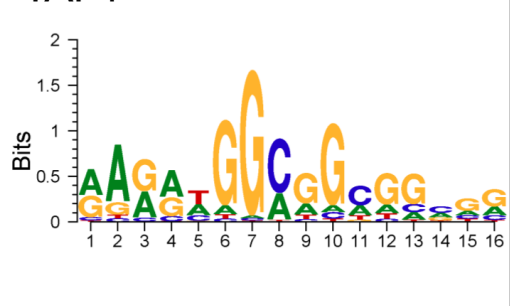
**MITF**



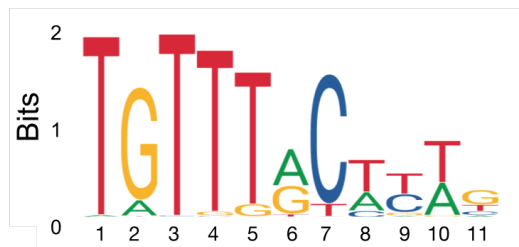
**SP2**



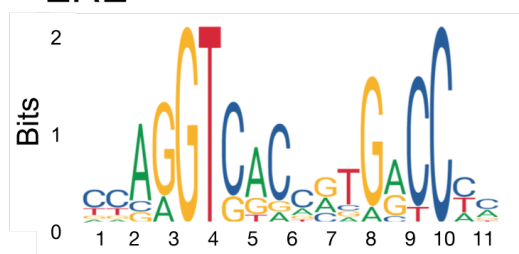
**TAF1**



**FOXA1**



**ERE**



**AP1 fos::jun**

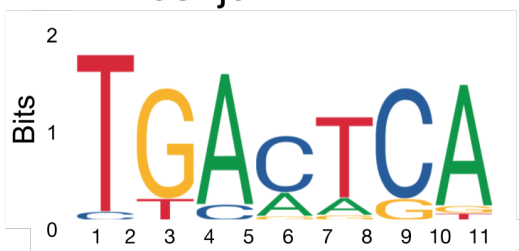


**Table 2.**

Family	Function	tRNAs	ed_activity	dox_activity	fox_fold	h3_fold
ALOXE	Insulator <sup>27,29</sup>	tRNA-Lys-TTT-3-5	Active	1	1.58	0.76
		tRNA-Gln-CTG-1-5	Inactive	0	1.73	0.80
		tRNA-Leu-TAG-1-1	Active	1	1.56	1.04
		tRNA-Arg-TCT-2-1	Active	1	1.29	1.15
Ebersole Insulator <sup>28,29</sup>		tRNA-Glu-CTC-1-5	Active	1	0.92	1.01
		tRNA-Gly-TCC-2-5	Active	1	0.94	1.27
		tRNA-Asp-GTC-2-5	Active	1	0.86	1.58
		tRNA-Leu-CAG-1-5	Inactive	0	0.67	1.03
HES7	Proximate to ALOXE	tRNA-Gly-GCC-2-6	Active	1	1.17	0.86
Per1	Per1	tRNA-Ser-CGA-1-1	Active	1	1.44	1.05
		tRNA-Thr-AGT-5-1	Active	1	1.39	0.99
TMEM10Δinsulator <sup>27,29</sup>		tRNA-Trp-CCA-3-3	Active	1	1.11	0.72
		tRNA-Ser-GCT-4-3	Active	1	1.10	0.66
		tRNA-Thr-AGT-1-1	Active	1	1.25	0.74
		tRNA-Ile-AAT-5-5	Active	1	1.16	0.83
Arg-CCG	Cancer Progression <sup>24</sup>	tRNA-Arg-CCG-1-1	Inactive	0	1.85	0.26
		tRNA-Arg-CCG-1-2	Inactive	0	0.57	0.49
		tRNA-Arg-CCG-1-3	Active	1	0.84	0.66

Family	Function	tRNAs	ed_activity	dox_activity	fox_fold	h3_fold
Glu-TTC	Cancer Progression <sup>24</sup>	tRNA-Arg-CCG-2-1	Active	1	0.88	0.32
		tRNA-Glu-TTC-1-1	Inactive	0	1.13	0.74
		tRNA-Glu-TTC-1-2	Active	1	0.87	0.98
		tRNA-Glu-TTC-2-1	Active	1	1.16	0.93
		tRNA-Glu-TTC-2-2	Active	1	1.55	0.94
		tRNA-Glu-TTC-4-2	Inactive	0	1.06	0.76
iMET	Translation Initiation	tRNA-iMet-CAT-1-1	Active	1	1.39	0.72
		tRNA-iMet-CAT-1-2	Active	1	1.01	0.55
		tRNA-iMet-CAT-1-3	Active	1	1.18	0.84
		tRNA-iMet-CAT-1-4	Inactive	0	1.26	0.52
		tRNA-iMet-CAT-1-5	Inactive	0	2.29	1.12
		tRNA-iMet-CAT-1-6	Inactive	0	1.71	1.73
		tRNA-iMet-CAT-1-7	Active	1	1.29	0.63
		tRNA-iMet-CAT-1-8	Active	1	1.40	0.75
		tRNA-iMet-CAT-2-1	Inactive	0	1.38	1.35
		tRNA-Met-CAT-1-1	Inactive	0	1.90	0.99
Met	iMet Control	tRNA-Met-CAT-2-1	Inactive	0	0.59	1.32
		tRNA-Met-CAT-3-1	Active	1	4.26	2.06

Family	Function	tRNAs	ed_activity	dox_activity	fox_fold	h3_fold
SeC	REDOX <sup>60</sup>	tRNA-Met-CAT-3-2	Inactive	0	1.24	0.24
		tRNA-Met-CAT-4-1	Inactive	0	1.30	1.26
		tRNA-Met-CAT-4-2	Inactive	0	0.74	1.27
		tRNA-Met-CAT-4-3	Active	1	1.46	1.55
		tRNA-Met-CAT-5-1	Inactive	0	0.48	1.17
		tRNA-Met-CAT-6-1	Active	1	1.07	0.79
		tRNA-Met-CAT-7-1	Inactive	0	0.85	0.65
		tRNA-SeC-TCA-1-1	Active	1	0.54	0.39
		tRNA-SeC-TCA-2-1	Inactive	0	1.38	1.92

## Discussion

- fox binding upstream = h3k27ac binding downstream
  - { briefly reiterate results
  - { binding intensity decreases
- Loses fox = weak binding?
- explain input peak
- Dynamic vs stable marks
- motifs interaction with ERa
- foxa1 looping

Future -

- ATAC-seq
- h3kme3 along with h3k27ac
- look at DN tdnas

## Conclusion

2627 Words

---

## References

- 1 Vannini A, Cramer P. Conservation between the RNA Polymerase I, II, and III Transcription Initiation Machineries. *Molecular Cell* 2012; **45**: 439–446.
- 2 Dieci G, Fiorino G, Castelnuovo M, Teichmann M, Pagano A. The expanding RNA polymerase III transcriptome. *Trends in Genetics* 2007; **23**: 614–622.
- 3 Raha D, Wang Z, Moqtaderi Z, Wu L, Zhong G, Gerstein M et al. Close association of RNA polymerase II and many transcription factors with Pol III genes. *Proceedings of the National Academy of Sciences* 2010; **107**: 3639–3644.
- 4 Schramm L, Hernandez N. Recruitment of RNA polymerase III to its target promoters. *Genes & Development* 2002; **16**: 2593–2620.
- 5 Lassar AB, Martin PL, Roeder RG. Transcription of Class III Genes: Formation of Preinitiation Complexes. *Science* 1983; **222**: 740–748.
- 6 Galli G, Hofstetter H, Birnstiel ML. Two conserved sequence blocks within eukaryotic tRNA genes are major promoter elements. *Nature* 1981; **294**: 626–631.
- 7 Schramm L, Pendergrast PS, Sun Y, Hernandez N. Different human TFIIB activities direct RNA polymerase III transcription from TATA-containing and TATA-less promoters. *Genes & Development* 2000; **14**: 2650–2663.
- 8 Khoo B, Brophy B, Jackson SP. Conserved functional domains of the RNA polymerase III general transcription factor BRF. *Genes & Development* 1994; **8**: 2879–2890.
- 9 Kassavetis GA, Braun BR, Nguyen LH, Peter Geiduschek E. *S. cerevisiae* TFIIB is the transcription initiation factor proper of RNA polymerase III, while TFIIA and TFIIC are assembly factors. *Cell* 1990; **60**: 235–245.
- 10 Brooks RF. Continuous protein synthesis is required to maintain the probability of entry into S phase. *Cell* 1977; **12**: 311–317.
- 11 Baxter GC, Stanners CP. The effect of protein degradation on cellular growth characteristics. *Journal of cellular physiology* 1978; **96**: 139–145.
- 12 Zetterberg A, Killander D. Quantitative cytophotometric and autoradiographic studies on the rate of protein synthesis during interphase in mouse fibroblasts in vitro. *Experimental cell research* 1965; **40**: 1–11.

- 13 Zhang Z, Ye Y, Gong J, Ruan H, Liu C-J, Xiang Y et al. Global analysis of tRNA and translation factor expression reveals a dynamic landscape of translational regulation in human cancers. *Communications biology* 2018; **1**: 234.
- 14 Pavon-Eternod M, Gomes S, Geslain R, Dai Q, Rosner MR, Pan T. tRNA over-expression in breast cancer and functional consequences. *Nucleic acids research* 2009; **37**: 7268–7280.
- 15 Winter AG, Sourvinos G, Allison SJ, Tosh K, Scott PH, Spandidos DA et al. RNA polymerase III transcription factor TFIIIC2 is overexpressed in ovarian tumors. *Proceedings of the National Academy of Sciences of the United States of America* 2000; **97**: 12619–12624.
- 16 Krishnan P, Ghosh S, Wang B, Heyns M, Li D, Mackey JR et al. Genome-wide profiling of transfer RNAs and their role as novel prognostic markers for breast cancer. *Scientific reports* 2016; **6**: 32843.
- 17 White RJ, Trouche D, Martin K, Jackson SP, Kouzarides T. Repression of RNA polymerase III transcription by the retinoblastoma protein. *Nature* 1996; **382**: 88–90.
- 18 Cairns CA, White RJ. p53 is a general repressor of RNA polymerase III transcription. *The EMBO journal* 1998; **17**: 3112–3123.
- 19 Sutcliffe JE, Brown TR, Allison SJ, Scott PH, White RJ. Retinoblastoma protein disrupts interactions required for RNA polymerase III transcription. *Molecular and cellular biology* 2000; **20**: 9192–9202.
- 20 Crighton D, Woiwode A, Zhang C, Mandavia N, Morton JP, Warnock LJ et al. p53 represses RNA polymerase III transcription by targeting TBP and inhibiting promoter occupancy by TFIIIB. *The EMBO journal* 2003; **22**: 2810–2820.
- 21 Gomez-Roman N, Grandori C, Eisenman RN, White RJ. Direct activation of RNA polymerase III transcription by c-myc. *Nature* 2003; **421**: 290–294.
- 22 Felton-Edkins ZA, Fairley JA, Graham EL, Johnston IM, White RJ, Scott PH. The mitogen-activated protein (MAP) kinase ERK induces tRNA synthesis by phosphorylating TFIIIB. *The EMBO journal* 2003; **22**: 2422–2432.
- 23 Kuchino Y, Borek E. [Tumour-specific phenylalanine tRNA contains two supernumerary methylated bases](#). *Nature* 1978; **271**: 126–129.
- 24 Goodarzi H, Nguyen HCB, Zhang S, Dill BD, Molina H, Tavazoie SF. [Modulated Expression of Specific tRNAs Drives Gene Expression and Cancer Progression](#). *Cell* 2016; **165**: 1416–1427.
- 25 Pavon-Eternod M, Gomes S, Rosner MR, Pan T. [Overexpression of initiator methionine tRNA leads to global reprogramming of tRNA expression and increased proliferation in human epithelial cells](#). *RNA* 2013; **19**: 461–466.
- 26 Birch J, Clarke CJ, Campbell AD, Campbell K, Mitchell L, Liko D et al. The initiator methionine tRNA drives cell migration and invasion leading to increased metastatic potential in melanoma. *Biology open* 2016; **5**: 1371–1379.
- 27 Raab JR, Chiu J, Zhu J, Katzman S, Kurukuti S, Wade PA et al. [Human tRNA genes function as chromatin insulators](#). *The EMBO Journal* 2011; **31**: 330–350.
- 28 Ebersole T, Kim J-H, Samoshkin A, Kouprina N, Pavlicek A, White RJ et al. [tRNA genes protect a reporter gene from epigenetic silencing in mouse cells](#). *Cell Cycle* 2011; **10**: 2779–2791.
- 29 Sizer RE, Chahid N, Butterfield SP, Donze D, Bryant NJ, White RJ. [TFIIC-based chromatin insulators through eukaryotic evolution](#). *Gene* 2022; **835**: 146533.
- 30 Sung H, Ferlay J, Siegel RL, Laversanne M, Soerjomataram I, Jemal A et al. Global cancer statistics 2020: GLOBOCAN estimates of incidence and mortality worldwide for 36 cancers in 185 countries. *CA: a cancer journal for clinicians* 2021; **71**: 209–249.

- 31 Allred DC, Brown P, Medina D. The origins of estrogen receptor alpha-positive and estrogen receptor alpha-negative human breast cancer. *Breast Cancer Research* 2004; **6**: doi:[10.1186/bcr938](https://doi.org/10.1186/bcr938).
- 32 Johnston SJ, Cheung K-L. Endocrine therapy for breast cancer: A model of hormonal manipulation. *Oncology and therapy* 2018; **6**: 141–156.
- 33 Anurag M, Ellis MJ, Haricharan S. DNA damage repair defects as a new class of endocrine treatment resistance driver. *Oncotarget* 2018; **9**: 36252–36253.
- 34 Costa RH, Grayson DR, Darnell JE Jr. Multiple hepatocyte-enriched nuclear factors function in the regulation of transthyretin and alpha 1-antitrypsin genes. *Molecular and cellular biology* 1989; **9**: 1415–1425.
- 35 Cirillo LA, Lin FR, Cuesta I, Friedman D, Jarnik M, Zaret KS. Opening of compacted chromatin by early developmental transcription factors HNF3 (FoxA) and GATA-4. *Molecular cell* 2002; **9**: 279–289.
- 36 Carroll JS, Liu XS, Brodsky AS, Li W, Meyer CA, Szary AJ et al. [Chromosome-Wide Mapping of Estrogen Receptor Binding Reveals Long-Range Regulation Requiring the Forkhead Protein FoxA1](#). *Cell* 2005; **122**: 33–43.
- 37 Laganière J, Deblois G, Lefebvre C, Bataille AR, Robert F, Giguère V. [Location analysis of estrogen receptor target promoters reveals that FOXA1 defines a domain of the estrogen response](#). *Proceedings of the National Academy of Sciences* 2005; **102**: 11651–11656.
- 38 Hurtado A, Holmes KA, Ross-Innes CS, Schmidt D, Carroll JS. FOXA1 is a key determinant of estrogen receptor function and endocrine response. *Apollo - University of Cambridge Repository* 2021. doi:[10.17863/CAM.63405](https://doi.org/10.17863/CAM.63405).
- 39 Wolf I, Bose S, Williamson EA, Miller CW, Karlan BY, Koeffler HP. FOXA1: Growth inhibitor and a favorable prognostic factor in human breast cancer. *International journal of cancer Journal international du cancer* 2007; **120**: 1013–1022.
- 40 Williamson EA, Wolf I, O'Kelly J, Bose S, Tanosaki S, Koeffler HP. BRCA1 and FOXA1 proteins coregulate the expression of the cell cycle-dependent kinase inhibitor p27(Kip1). *Oncogene* 2006; **25**: 1391–1399.
- 41 Tsuchiya A, Zhang GJ, Kanno M. Prognostic impact of cyclin-dependent kinase inhibitor p27kip1 in node-positive breast cancer. *Journal of surgical oncology* 1999; **70**: 230–234.
- 42 Fredersdorf S, Burns J, Milne AM, Packham G, Fallis L, Gillett CE et al. High level expression of p27<sup>kip1</sup> and cyclin D1 in some human breast cancer cells: Inverse correlation between the expression of p27<sup>kip1</sup> and degree of malignancy in human breast and colorectal cancers. *Proceedings of the National Academy of Sciences* 1997; **94**: 6380–6385.
- 43 Badve S, Turbin D, Thorat MA, Morimiya A, Nielsen TO, Perou CM et al. FOXA1 expression in breast cancer—correlation with luminal subtype a and survival. *Clinical cancer research: an official journal of the American Association for Cancer Research* 2007; **13**: 4415–4421.
- 44 Ross-Innes CS, Stark R, Teschendorff AE, Holmes KA, Ali HR, Dunning MJ et al. [Differential oestrogen receptor binding is associated with clinical outcome in breast cancer](#). *Nature* 2012; **481**: 389–393.
- 45 Fu X, Jeselsohn R, Pereira R, Hollingsworth EF, Creighton CJ, Li F et al. FOXA1 overexpression mediates endocrine resistance by altering the ER transcriptome and IL-8 expression in ER-positive breast cancer. *Proceedings of the National Academy of Sciences of the United States of America* 2016; **113**: E6600–E6609.
- 46 Hah N, Danko CG, Core L, Waterfall JJ, Siepel A, Lis JT et al. A rapid, extensive, and transient transcriptional response to estrogen signaling in breast cancer cells. *Cell* 2011; **145**: 622–634.
- 47 Zhong Q, Shi G, Zhang Q, Lu L, Levy D, Zhong S. [Tamoxifen represses alcohol-induced transcription of RNA polymerase III-dependent genes in breast cancer cells](#). *Oncotarget* 2014; **5**: 12410–12417.

- 48 Fu X, Pereira R, De Angelis C, Veeraraghavan J, Nanda S, Qin L et al. FOXA1 upregulation promotes enhancer and transcriptional reprogramming in endocrine-resistant breast cancer. *Proceedings of the National Academy of Sciences* 2019; **116**: 26823–26834.
- 49 Leinonen R, Sugawara H, Shumway M. The Sequence Read Archive. *Nucleic Acids Research* 2010; **39**: D19–D21.
- 50 Afgan E, Nekrutenko A, Grüning BA, Blankenberg D, Goecks J, Schatz MC et al. The Galaxy platform for accessible, reproducible and collaborative biomedical analyses: 2022 update. *Nucleic Acids Research* 2022; **50**: W345–W351.
- 51 Langmead B, Salzberg SL. Fast gapped-read alignment with Bowtie 2. *Nature Methods* 2012; **9**: 357–359.
- 52 Karolchik D. The UCSC Table Browser data retrieval tool. *Nucleic Acids Research* 2004; **32**: 493D–496.
- 53 Chan PP, Lowe TM. GtRNAdb 2.0: an expanded database of transfer RNA genes identified in complete and draft genomes. *Nucleic Acids Research* 2015; **44**: D184–D189.
- 54 Lerdrup M, Johansen JV, Agrawal-Singh S, Hansen K. An interactive environment for agile analysis and visualization of ChIP-sequencing data. *Nature Structural & Molecular Biology* 2016; **23**: 349–357.
- 55 R Core Team. *R: A language and environment for statistical computing*. R Foundation for Statistical Computing: Vienna, Austria, 2023. <https://www.R-project.org/>.
- 56 Wickham H, Averick M, Bryan J, Chang W, McGowan L, François R et al. Welcome to the tidyverse. *Journal of Open Source Software* 2019; **4**: 1686.
- 57 Kassambara A. Ggpubr: 'ggplot2' based publication ready plots. 2023 <https://CRAN.R-project.org/package=ggpubr>.
- 58 Fu X, Jeselsohn R, Pereira R, Hollingsworth EF, Creighton CJ, Li F et al. FOXA1 overexpression mediates endocrine resistance by altering the ER transcriptome and IL-8 expression in ER-positive breast cancer. *Proceedings of the National Academy of Sciences* 2016; **113**. doi:10.1073/pnas.1612835113.
- 59 Torres AG. Enjoy the Silence: Nearly Half of Human tRNA Genes Are Silent. *Bioinformatics and Biology Insights* 2019; **13**: 117793221986845.
- 60 Sangha AK, Kantidakis T. The Aminoacyl-tRNA Synthetase and tRNA Expression Levels Are Deregulated in Cancer and Correlate Independently with Patient Survival. *Current Issues in Molecular Biology* 2022; **44**: 3001–3019.